IJE TRANSACTIONS B: Application Vol. 26, No. 8, (August 2013) 913-926

International Journal of Engineering

Journal Homepage: www.ije.ir

Energy and Exergy Analysis of Air PV/T Collector of Forced Convection with and without Glass Cover

A. B. Kasaeian[a] *, M. Dehghani Mobarakeh[b], S. Golzari[a], M. M. Akhlaghi[a]

[a] Faculty of New Science & Technologies, University of Tehran, Tehran, Iran
[b] Research Institute of Petroleum Industry, Tehran, Iran

PAPER INFO

Paper history:
Received 08 December 2012
Received in revised form 06 February 2013
Accepted 28 February 2013

Keywords:
Air PV/T Collector
Energy Efficiency
Exergy Efficiency

ABSTRACT

In this study, the overall performance of air PV/T, based on energy and exergy analysis has been investigated. Two combinations of air PV/T, which consist of unglazed and glazed air PV/T, are considered. Thermal analysis and numerical calculations were carried out, and the performance parameters of the system for the climate conditions of Kerman were studied. The results are presented in graphs and some parameters such as electrical, thermal and overall energy and exergy efficiencies of these two combinations, have been compared. The results show higher thermal and overall energy efficiencies of glazed PV/T, whereas, higher electrical and overall exergy efficiencies of unglazed one were observed. The overall energy efficiency of glazed and unglazed systems are about 66% and 52%, respectively. Also, the overall exergy efficiency for unglazed and glazed systems is between 11.2-11.6% and 10.5-11.1% respectively.

doi: *10.5829/idosi.ije.2013.26.08b.13*

NOMENCLATURE

A	Area	T	Temperature
b	The width of PV/T collector	U_b	An overall back loss coefficient from flowing air to ambient (W/m^2K)
C	Specific heat capacity(kj/kgK)	U_L	An overall heat transfer coefficient from air PV/T to ambient (W/m^2K)
dx	Element length of flow duct	U_t	An overall heat transfer coefficient from solar cell to ambient through glass cover (W/m^2K)
$\dot{E}x$	Exergy rate(W)	U_T	A conductive overall heat transfer coefficient from solar cell to flowing air through Tedlar (W/m^2K)
h	Heat transfer coefficient	U_{tT}	An overall heat transfer coefficient from glass to Tedlar through solar cell (W/m^2K)
I	Circuit current(A)	U_{ta}	An overall heat transfer coefficient from glass to air through solar cell and Tedlar(W/m^2K)
I (t)	Solar radiation intensity(W/m^2)	V	Circuit Voltage(V), Wind speed(m/s)
k	Thermal conductivity(W/mK)		
L	The length of PV/T collector	**Greek Symbols**	
$\dot{m}$	Mass flow rate of air(kg/s)	α	absorptivity
Nu	Nusselt number	β	packing factor
Pr	Prandtl number	ε	emissivity
PV	Photovoltaic	η	efficiency
$\dot{Q}$	Heat transfer rate	ρ	density
R	Resistance (Ω)	σ	Stefan-Boltzmann's constant (W/m^2K^4)
Ra	Rayleigh number	δ	duct depth
Re	Reynolds number	μ	temperature coefficient

* Corresponding Author Email: akasa@ut.ac.ir (A. B. Kasaeian)

Subscript			
a	ambient	oc	open-circuit
b	bottom	out	outlet
bs	back surface of Tedlar	ov	overall
c	solar cell	r	radiation
conv	convection	ref	reference
des	destruction	sc	short-circuit
el	electrical	sh	shunt
ex	exergy	t	top
g	glass	T	Tedlar
G	glaze	th	thermal
i	insulation	u	useful
in	inlet	w	wind
mp	maximum power point		

1. INTRODUCTION

Regarding the environmental problems caused by the use of fossil energies, renewable energy has been proposed as an effective solution. Solar energy is a great and helpful source and due to its availability in most parts of the world, it is one of the most important kinds of these energies. Among all types of solar energy facilities, the photovoltaic solar energy (PV) was selected for our study.

A common PV module converts 4–17% of the incoming solar radiation into electricity, depending on the type of the solar cells in use and the working conditions. In other words, more than 50% of the incident solar energy is converted as heat (after deducting the reflected portion). This may lead to extreme cell working temperature as much as 50°C above the ambient environment. There can be two undesirable consequences: (i) a drop in cell efficiency (typically 0.4% per °C rise for C-Si cells), and (ii) a permanent structural damage of the module if the thermal stress remains for prolonged period [1].

By cooling the solar cell with circulating fluid such as water or air, electricity generation can be increased. However, a better design is to use the heat extracted by the fluid. and increase the energy yield per square meter of the solar panel. This design can be very effective and efficient for areas where solar radiation is available, but mostly the available area is limited. So, the PV/T system is the technology that is developed for satisfy this purpose.

PV/T technology with a combination of photovoltaic and solar thermal systems, can simultaneously convert solar radiation to electricity and heat. In this system, PV module that is coupled to solar-thermal, converts part of solar radiation into electricity; the remaining part causes PV heating up the module, and the produced heat is extracted by a coolant fluid in the thermal system to harness thermal energy, while at the same time, the PV temperature is decreased and electricity yield is increased. The applications of this system, beside electricity generation, are in heating such as hot water and space heating for buildings.

Both air and water have been used as heat transfer fluids in PV/T solar collectors which are known as PVT/air and PVT/water systems respectively. Kern and Russell introduced the main concepts of these systems with results for the cases of water or air as coolant in 1970's [1]. During the past 40 years, the performance of PV/T systems has been studied using experimental and numerical methods. Hagazy [2] investigated a glazed photovoltaic/thermal air system for a single and a double pass air heater for space heating and the drying purposes. Zondag et al. [3] developed 1D, 2D, and 3D dynamical models of a multi-panel (PV/T) in 2002. They concluded that the simple 1D steady-state model for computing the daily yield of the multi-panel, can behave as precise as the time consuming 2D and 3D dynamic models. Tiwari et al. [4] evaluated the performance of PV/T air system for different climate conditions of India. Theoretical analysis and experimental validations have also been carried out. A fair agreement can be observed between the theoretical results and the practical works. Tiwari and Sodha [5] in 2006 evaluated the overall performance of various configurations of hybrid PV/T thermal air collector for different weather of New Delhi, and experimental validation has been carried out.

In 2007, Alfegi et al. [6] investigated a double duct PV/T air system experimentally with fin, to increase heat transfer, and with compound parabolic

concentrating, to concentrate solar radiation on solar cells. In the same year, Othman et al. [7] studied numerically the performance of one similar system numerically. For the purpose of achieving a higher thermal output and more PV cooling, Tonui and Tripanagnostopoulos [8] in 2007, studied the performance of two low cost heat extraction improvement modifications in the channel of a PV/T system. Using a thin flat metal sheet suspended at the middle and finned back wall of an air channel in the PV/T air configuration, they managed to keep the electrical efficiency at a reasonable level.

In 2009, Joshi et al. [9] developed a thermal model for the PV module integrated with solar air collector and validated it experimentally. They indicated that the PV module temperature can be controlled and reduced in consequence of changing the mass flow rate of air in solar collector and the efficiency of PV module can be increased. Solanki et al. in 2009 accomplished the thermal and electrical testing of PV/T air collector by developing an indoor standard test procedure in a steady state condition [10]. Jin et al. [11] developed a single pass PV/T with rectangle tunnel absorber in 2010. The rectangle tunnel functioned as an absorber and was positioned at the back side of a standard photovoltaic panel. According to their conclusion, the hybrid PV/T with rectangle tunnel as heat absorber has higher performance compared to the conventional PV/T system. Sarhhadi et al. [12] investigated the thermal and electrical performance of a solar photovoltaic thermal (PV/T) air collector in 2010. In order to amend the thermal model of a PV/T air collector, some modifications have been carried out on the heat loss coefficients. Chow did a review on the PV/T hybrid solar technology especially the air collector systems. His report, in particular, states the advancements in recent years and the required works of future [1].

Most studies have examined the system from the viewpoint of energy, but exergy analysis offers more real and practical aspects of the process. Joshi and Tiwari [13] evaluated exergy and energy analysis of PVT air system for cold climate of India in 2007. They reported an instantaneous energy and exergy efficiencies between 55-65% and 12-15%, respectively. Chow et al. [14] developed energy and exergy analysis of PVT/water with and without glass cover in 2009. Their numerical model results indicate the higher energy efficiency for a model with a glass cover, but the exergy efficiency is greater for the model without cover. In 2009, exergy analysis of integrated photovoltaic thermal solar water heater under constant flow rate and constant collection temperature modes has been investigated by Tiwari et al. [15]. Dubey et al. [16] evaluated the energy and exergy performance of a PV/T air collector with air duct above the absorber plate and the one with air duct below the absorber plate. They investigated the effect of design and operating parameters at four weather conditions on the performance of the aforementioned PV/T air collectors for five different cities of India. They found that the latter gives better results in terms of thermal energy, electrical energy and exergy gain.

Agrawal and Tiwari [17] evaluated energy and exergy of a hybrid micro-channel photovoltaic thermal module under constant mass flow rate of air. On the basis of numerical computations, their results indicate that the overall thermal and exergy efficiency have been increased in this system. In 2010, Sarhaddi et al. [18] evaluated the exergy performance of solar photovoltaic thermal (PV/T) air collector. The results show that the overall exergy efficiency and energy efficiency are about 45 and 10.75%, respectively for an unglazed PV/T model. In the same year, Shahsavar et al. [19] analyzed the energy and the exergy performance of a PV/T air collector which was ventilated naturally. The metal sheet was suspended at the middle of an air channel in their studied PV/T air configuration. The results indicate that the exergy and energy efficiencies for the unglazed model are approximately 9 and 8%, respectively. Also, the exergy and energy efficiencies for the glazed model were reported 7 and 11%, respectively.

Most of the studies on the energy and exergy performance of PV/T have analyzed water PV/T collectors. Sarhaddi et al. [18] evaluated the exergy performance of a common model of unglazed air PV/T with forced air flow. In this paper, an attempt has been made to evaluate the energy and exergy efficiencies of the following configurations of air PV/T systems which are the typical air PV/T systems. We investigate the effect of glass cover on the energy and exergy efficiencies of air PV/T system with forced air flow for the climate of Kerman. In terms of intensity of solar radiation and sunshine hours, Kerman is one of the best places in Iran. Two types of glass cover used are:

a) unglazed glass-to-Tedlar air PV/T, Model I, Figure 1(a).
b) glazed glass-to-Tedlar air PV/T, Model II, Figure 1(b).

2. THEORETICAL ANALYSIS

Some parameters on exergy analysis are dependent on energy analysis. At first, the energy analysis is performed. To determine temperature of components of PV/T, an energy balance equation should be written for each component. The following assumptions are considered in order to write energy balance [5, 7, 9]:

1. The system is in the quasi-steady state condition.
2. One-dimensional heat conduction is considered.
3. The temperature variation along the thickness of component is neglected.
4. The air flow through air duct is in forced mode.

5. The transmissivity of ethylene-vinyl acrylate material (EVA) is nearly 100%.
6. The heat capacity of the components except for the air, are neglected.

With these assumptions, the energy balance equations based on the thermal resistance circuit diagram of each case as shown in Figure 1 can be written in section (2.1). A differential element with the length of 'dx' as shown in Figure 2 is considered.

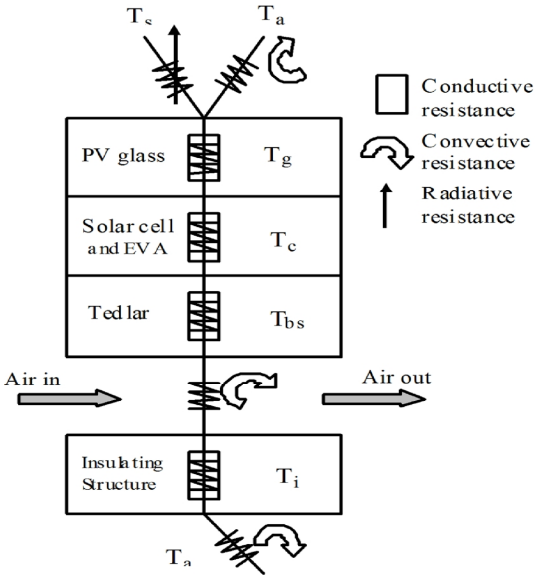

1(a)

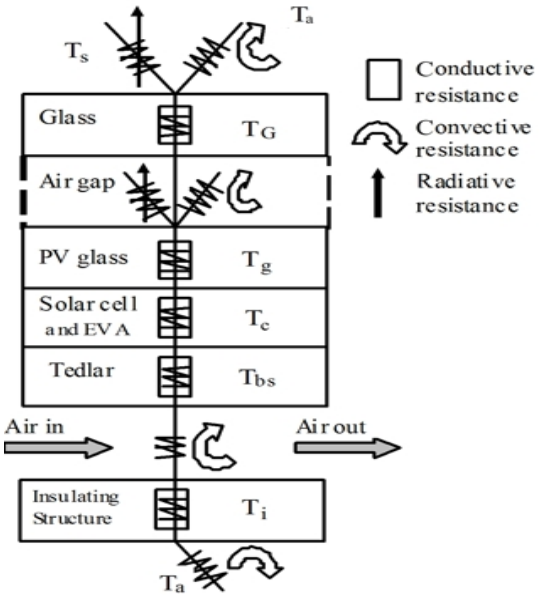

1(b)

Figure 1. (a) Thermal resistance circuit diagram for unglazed air PV/T (Model I). (b) Thermal resistance circuit diagram for glazed air PV/T (Model II). [4, 5,12]

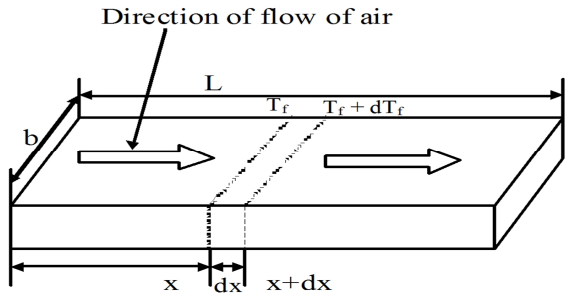

Figure 2. The cross-sectional view of an element with the length of 'dx' showing the flow pattern of air below Tedlar [9, 12, 13]

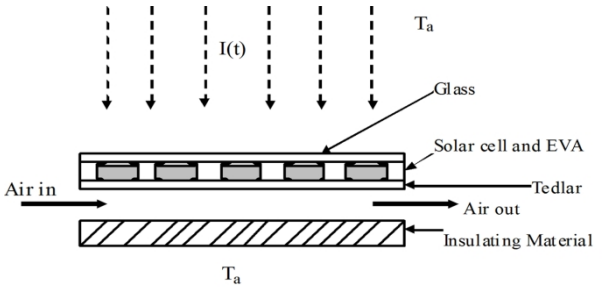

Figure 3. The cross-sectional view of unglazed glass-to-Tedlar air PV/T [12]

2. 1. Model I. PV/T Air System without Glazing Cover (unglazed) The cross-sectional view of model I is shown in Figure 3. The energy balance equations of the component are as follow [5,10,13]:

- For solar cell module

$$T_g[\alpha_c\beta_c I(t) + (1-\beta_c)\alpha_T I(t)]\,bdx = [U_t(T_c - T_a) + U_T(T_c - T_{bs})]bdx + \eta_c I(t)\beta_c bd \quad (1)$$

From Equation (1), the expression for cell temperature is:

$$T_c = \frac{(\tau\alpha)_{eff} I(t) + U_t T_a + U_T T_{bs}}{U_t + U_T} \quad (2)$$

- For the back surface of Tedlar

$$U_T(T_c - T_{bs})bdx = h_{air}(T_{bs} - T_{air})bdx \quad (3)$$

Using Equations (2) and (3), the expression for back surface temperature of PV module can be obtained as

$$T_{bs} = \frac{h_{p1}(\tau\alpha)_{eff} I(t) + U_{tT} T_a + h_{air} T_{air}}{U_{tT} + h_{air}} \quad (4)$$

where, h_{p1}, is the penalty factor due to the presence of solar cell material, Tedlar and EVA. Also, $(\tau\alpha)_{eff}$ is the effective transmission-absorption. They are given by:

$$h_{p1} = \frac{U_T}{U_T + U_t} \quad (5)$$

$$(\tau\alpha)_{\text{eff}} = \tau_g[\alpha_c\beta_c + (1-\beta_c)\alpha_T - \eta_c\beta_c] \quad (6)$$

- For air flowing below the Tedlar

$$T_g[\alpha_c\beta_c I(t) + (1-\beta_c)\alpha_T I(t)]\,bdx = [U_t(T_c - T_a) + U_T(T_c - T_{bs})]bdx + \eta_c I(t)\beta_c bd \quad (7)$$

The overall heat loss coefficient for PV/T is given by:

$$U_L = U_{ta} + U_b \quad (8)$$

The other heat loss coefficients that are used in the above equations are taken from Table 1.

2. 2. Model II. PV/T Air System with Glazing Cover (glazed) The cross-sectional view of model II is shown in Figure 4.

- For glazing cover:

$$\alpha_G I(t)bdx = [(h_{r,cG} + h_{conv,cG})(T_G - T_c) + (h_{conv,t} + h_{r,Gs})(T_G - T_a)]bdx \quad (9)$$

- For the solar cell module:

Same as in Equation (1) with the changes in U_t as follows:

$$U_t = \left[\frac{L_g}{K_g} + \frac{1}{h_{r,cg}+h_{conv,cg}} + \frac{L_G}{K_G} + \frac{1}{h_{conv,t}+h_{r,gs}}\right]^{-1} \quad (10)$$

- For the back surface of the Tedlar same as Equation (3)
- For the air flowing below the Tedlar same as Equation (5)

TABLE 1. The relations for heat loss coefficients

$U_{ta} = \left[\frac{1}{U_{tT}} + \frac{1}{h_{air}}\right]^{-1}$	$U_T = \frac{K_T}{L_T}$
$U_b = \left[\frac{L_i}{K_i} + \frac{1}{h_{conv,b}}\right]^{-1}$	$U_t = \left[\frac{L_g}{K_g} + \frac{1}{h_{conv,t}+h_{r,cs}}\right]^{-1}$
$U_{tT} = \left[\frac{1}{U_T} + \frac{1}{U_t}\right]^{-1}$	

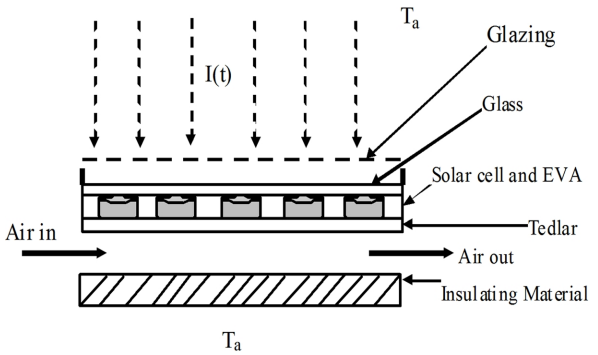

Figure 4. The cross-sectional view of glazed glass-to-Tedlar air PV/T

2. 3. The Radiative and Convective Heat Transfer Coefficients The radiative and convective heat transfer coefficients in the above equations are calculated by following relations which are taken from references [2, 3, 8] . The radiative heat transfer coefficients from solar cell to ambient through glass cover in model I is taken as:

$$h_{r,cs} = \varepsilon_g\sigma\left(T_c^4 - T_{sky}^4\right)/(T_c - T_a) \quad (11)$$

The effective temperature of the sky is calculated from the following empirical relation[8]:

$$T_{sky} = 0.0552T_a^{1.5} \quad (12)$$

The radiative heat transfer coefficients from glass cover to ambient in model II are considered as:

$$h_{r,Gs} = \varepsilon_G\sigma\left(T_G^4 - T_{sky}^4\right)/(T_G - T_a) \quad (13)$$

The convective heat transfer coefficients on the top and bottom surface of PV/T is calculated by [8] :

$$h_{conv,t} = 2.8 + 3V_w \quad (14)$$

$$h_{conv,b} = 2.8 + 3V_w \quad (15)$$

The parameter $h_{conv,cG}$ is the free convection heat transfer coefficient of the air gap between the PV module and the glass cover in model II. According to Hegazy [2] , it is computed by:

$$h_{conv,cG} = \frac{Nu_{air}K_{air}}{\delta_{air}} \quad (16)$$

$$Nu_{air_x} = \frac{1}{1+1.44\left[1-\frac{1708(sin1.8\varphi)^{1.6}}{Ra\cos\varphi}\right]\left[1-\frac{1708}{Ra\cos\varphi}\right]^{*}+\left[\left(\frac{Ra\cos\varphi}{5830}\right)^{1.3}-1\right]^{*}} \quad (17)$$

where, Ra is the air gap Rayleigh number (Ra= Gr*Pr), and φ the collector tilt angle (30 for Kerman). The notation [ ]* indicates that the term in the bracket will be considered in calculations if it is positive, but if this term is negative, zero will be used. All the properties are evaluated at the air gap mean temperature, $(T_c+T_g)/2$. Also, $h_{r,cG}$ is the radiative heat transfer coefficient from solar cell to glass cover in model II., that is computed by:

$$h_{r,cG} = \frac{\varepsilon_G\varepsilon_c}{\varepsilon_G+\varepsilon_c-\varepsilon_G\varepsilon_c}\sigma(T_c+T_G)(T_c^2+T_G^2) \quad (18)$$

It is supposed that two DC electric fans blow air into the air duct. These DC fans consume small amount of electricity, which is neglected during the simulation. The forced convective heat transfer coefficient (h_{air}) between the turbulent airflow and both the PV panel and the back plate is calculated according to the Nusselt number. The following correlation is used for calculating h_{air} [8]:

$$h_{air} = \frac{k}{D_H}\left\{0.0182\text{Re}^{0.8}\text{Pr}^{0.4}\left[1 + S\frac{D_H}{L}\right]\right\} \quad (19)$$

$S = 14.3\ \log(L/D_H) - 7.9$ for $0 < L/D_H \leq 60$

$S = 17.5$ for $L/D_H > 60$

3. CALCULATING METHOD

Substituting Equation (4) into Equation (7) can eliminate the variables T_{bs} from Equation (7), and give the following first-order linear differential equation for the outlet air temperature calculation:

$$\frac{dT_{air}}{dx} + \frac{U_L}{\dot{m}_{air}c_{air}}T_{air} = \frac{h_{p1}h_{p2}(\tau\alpha)_{eff}I(t) - U_L T_a}{\dot{m}_{air}c_{air}} \quad (20)$$

where, h_{p2}, is the penalty factor due to the presence of the interface between the Tedlar and the working fluid through the channel.

$$h_{p2} = \frac{h_{air}}{U_{tT} + h_{air}} \quad (21)$$

Integrating Equation (20) with boundary condition at x=0, $T_{air}=T_{airin}$ and x=L, $T_{air}=T_{airout}$ we get:

$$T_{airout} = \left(\frac{h_{p1}h_{p2}(\tau\alpha)_{eff}I(t)}{U_L} + T_a\right)\left(1 - exp\left(-\frac{U_L bL}{\dot{m}_{air}c_{air}}\right)\right) + T_{airin}exp\left(-\frac{U_L bL}{\dot{m}_{air}c_{air}}\right) \quad (22)$$

The average air temperature over the length of the air duct below PV module is obtained as:

$$\bar{T}_{air} = \frac{1}{L}\int_0^L T_{air}(x)dx = \left(\frac{h_{p1}h_{p2}(\tau\alpha)_{eff}I(t)}{U_L} + T_a\right)\left[\left(1 - exp\left(-\frac{U_L bL}{\dot{m}_{air}c_{air}}\right)\right)\Big/\frac{U_L bL}{\dot{m}_{air}c_{air}}\right] + T_{airin}\left(1 - exp\left(-\frac{U_L bL}{\dot{m}_{air}c_{air}}\right)\Big/\frac{U_L bL}{\dot{m}_{air}c_{air}}\right) \quad (23)$$

4. EVALUATION OF THE OVERALL PERFORMANCE

The system performance can be investigated from the different aspects such as thermodynamical, economical and environmental. In this section, the overall system performance based on both the first and second laws of thermodynamics is evaluated.

4. 1. Energy Analysis The main approach by the first law of thermodynamics is evaluating the quantity of energy. According to this law, by writing the energy balance mentioned in the previous section, thermal efficiency of the system can be calculated. The useful thermal energy gained by airflow through the PV/T system is:

$$\dot{Q}_u = \dot{m}_{air}c_{air}(T_{airout} - T_{airin}) \quad (24)$$

$$\dot{Q}_u = \frac{\dot{m}_{air}c_{air}}{U_L}[h_{p1}h_{p2}(\tau\alpha)_{eff}I(t) - U_L(T_{airin} - T_a)] \times \left[1 - exp\left(-\frac{U_L bL}{\dot{m}_{air}c_{air}}\right)\right] \quad (25)$$

- **Thermal Efficiency**

The thermal efficiency of the PV/T system based on the first law of thermodynamics is:

$$\eta_{th} = \frac{\dot{Q}_u}{bLI(t)} = \frac{\dot{m}_{air}c_{air}}{U_L bL}F_R\left[h_{p1}h_{p2}(\tau\alpha)_{eff}\frac{U_L(T_{airin} - T_a)}{I(t)}\right] \quad (26)$$

$$F_R = 1 - exp\left(-\frac{U_L bL}{\dot{m}_{air}c_{air}}\right) \quad (27)$$

where F_R is heat removal factor. This factor is an important design parameter, because it shows the thermal resistance that absorbs the solar radiation which is encountered in the path of reaching the fluid.

- **Electrical Efficiency**

An expression for the temperature dependent electrical efficiency of a PV module is given by:

$$\eta_{el} = \eta_{ref}[1 - \beta(T_c - T_{ref})] \quad (28)$$

where β=0.0045 $^{\circ}C^{-1}$ is the temperature coefficient, T_c the temperature of the cell, T_{ref} the reference temperature (taken as 25˚C) and η_{ref} the efficiency of the module at the reference temperature (taken as 0.12). [2,6,7,8]. Sarhaddi et al. [12] showed that Equation (28) has some deficiencies. According to their results, the electrical efficiency can be calculated by electrical simulation of PV module. For this purpose a five-parameter model is useful for the solar cell IV characteristic curve. The equivalent circuit of this model is shown in Figure 5. This model and its solution is provided by Duffi and Beckman [20], in which the relationship between voltage and current are defined as follows:

$$I = I_L - I_D - I_{sh} = I_L - I_o\{exp[(V + I.R_s)/a] - 1\} - \frac{V + I.R_s}{R_{sh}} \quad (29)$$

where I_L is the light current, I_D the diode current of the equivalent circuit, I_o the inverse polarization current, R_s the series resistance, R_{sh} the shunt resistance, and 'a' the curve fitting parameter. The shunt resistance of most modern cells is very large and the last term of Equation (29) can often be neglected [19,20] .

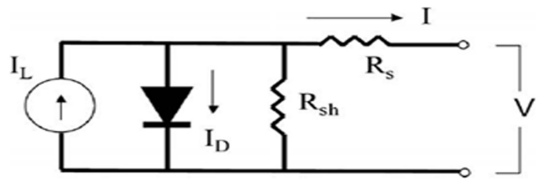

Figure 5. The equivalent circuit for a PV generator [12,18,19]

Therefore, Equation (29) may be reduced as follows:

$$I = I_L - I_D - I_{sh} = I_L - I_o\{exp[(V + I.R_s)/a] - 1\} \quad (30)$$

In order to determine the four parameters I_L, I_o, R_s and 'a' in the reference condition or SRC standard condition (solar radiation I_{ref}=1000 Wm^{-2}; solar cell temperature (T_c=25°C), four conditions are required as follows [12,20]:

At short circuit current: $I = I_{sc,ref}$, $V = 0$

At open circuit voltage: $I = 0$, $V = V_{oc,ref}$

At the maximum power point: $I = I_{mp,ref}$, $V = V_{mp,ref}$

At the maximum power point: $[d(IV)/dV]_{mp} = 0$

Performing experiments in the reference conditions, the manufacturers of photovoltaic modules offer the values of $V_{oc,ref}$, $I_{sc,ref}$, $I_{mp,ref}$ and $V_{mp,ref}$, the temperature coefficient of short circuit current ($\mu_{I,sc}$) and open circuit voltage ($\mu_{V,oc}$) for each photovoltaic module. With substituting four conditions into Equation (35), a non-linear system of equations is produced. To solve the nonlinear system of equations, the numerical methods such as Newton-Rafson can be used. By solving the system of equations, the unknown parameters are specified in the reference conditions [20]. In order to calculate the voltage and current in the new conditions (I_{new}, $T_{c,new}$) the equations of Duffi and Beckman [20] may be applied. In this study, MATLAB R2011a software is used to solve these equations. The reference parameters that are provided by the manufacturer, have been presented in Table 2.

By solving the model for the photovoltaic operating conditions used in this study the system's electrical efficiency can be calculated. The electrical efficiency of a PV module can be defined as the ratio of actual electrical output to input solar energy incident on PV surface area as follows [12,19].

$$\eta_{el} = \frac{V_{mp} I_{mp}}{S} \quad (31)$$

where S is the absorbed solar flux that is given by:

$$S = I(t)NsNmA_{cell} \quad (32)$$

where, A_{cell} is the PV module area, Nm and Ns are the number of the modules in series per string and number of strings, which are taken in this work as1 and 2, respectively.

- **Overall Efficiency**

The overall efficiency, which includes electrical and thermal, of PV/T system is:

$$S = I(t)NsNmA_{cell} \quad (33)$$

where, the 0.4 factor is the conversion factor from thermal energy to electrical energy of the thermal power plant [5,12]. In this case, an overall efficiency will be just thermal efficiency.

A computer program is written to evaluate the performance of the two systems in the climatic conditions. In order to calculate the performance parameters based on the temperature of the module layers of PV/T, the iteration method was applied. To start the calculations, an initial value is estimated for T_g, T_{airout}, T_c and T_{bs}. With the assumed temperature, in the first stage, the equations of heat transfer coefficients (Equations (16-24)) are solved. Then, by solving the energy equations (Equations (25-28)), the new temperatures are obtained. Substituting of the new values of temperatures in the equations, the next step is done. Similarly, the process continues until the temperature of various layers of the system is specified.

4. 2. Exergy Analysis With the first law of thermodynamics, one cannot have a comprehensive evaluation of the system. It isn't able to prefer a proper criterion to characterize the system because the thermal and electrical energy generated by the system are not the same in the terms of quality, even if they are equal in the terms of quantity. Electrical energy is the high-grade form of energy and thermal energy is the low-grade one. Exergy analysis that is based on the second law of thermodynamics, can evaluate the quality of energy.

The exergy of a thermodynamic system is the maximum work that can be done by the system when undergoes reversible processes that bring the system into complete thermodynamic equilibrium with a defined reference environment. Exergy is always destroy when a process involves a temperature change. This destruction is proportional to the entropy increase of the system together with its surroundings. The destroy exergy has been called anergy. Exergy analysis identifies the location, magnitude and the source of thermodynamic inefficiencies in a system. This information, which could not be provided by other means (e.g., energy analysis), is very useful for the improvement and cost-effectiveness of the system [17].

For exergy analysis, exergy balance which includes the rate of total exergy inflow, exergy outflow rate and exergy destruction rate from the system is as follows:

$$\sum \dot{E}x_{in} - \sum \dot{E}x_{out} = \sum \dot{E}x_{des} \quad (34)$$

$$\sum \dot{E}x_{in} - (\dot{E}x_{th} + \dot{E}x_{el}) = \sum \dot{E}x_{des} \quad (35)$$

where the nature of the rate of exergy inflow is radiation. There are some calculation methods based on this assumption, among which the Petela [21] method can be chosen and written as:

$$\sum \dot{E}x_{in} = \left[1 + \frac{1}{3}\left(\frac{T_a}{T_{sun}}\right)^4 - \frac{4T_a}{3T_{sun}}\right] I(t)A_{cell} \quad (36)$$

where T_{sun} is the sun surface temperature, 6000 K.

The total rate of exergy outflow is the rate of exergy obtained from the air in channel and the electrical exergy that are obtained as [16, 17].

$$\dot{E}x_{th} = Q_u \left[1 - \frac{T_a+273}{T_{air\ out}+273}\right] \quad (37)$$

$$\dot{E}x_{el} = \left[\frac{\eta_{el} A_{cell} I(t)}{1000}\right] \quad (38)$$

The thermal and electrical efficiencies of the second law can be calculated by:

$$\eta_{II,th} = \frac{\dot{E}x_{th}}{\sum \dot{E}x_{in}} \quad (39)$$

$$\eta_{II,el} = \frac{\dot{E}x_{el}}{\sum \dot{E}x_{in}} \quad (40)$$

Exergy efficiency of the second law, is defined as the ratio of the total produced exergy (exergy outflow) to the exergy inflow [16, 17]

$$\eta_{ex} = \frac{\sum \dot{E}x_{out}}{\sum \dot{E}x_{in}} = \frac{\dot{E}x_{th}+\dot{E}x_{el}}{\sum \dot{E}x_{in}} = \eta_{II,th} + \eta_{II,el} \quad (41)$$

5. RESULTS AND DISCUTION

The weather conditions, for one day in July 2009, are given in Table 2 [19] and some thermo-physical, operating and design parameters which are used in this study are presented in Table 3.

By solving the equations in terms of 0.1 kg/s mass flow rate and wind velocity at V_w=1 m/s, with the iteration procedure, the output air temperature (T_{airout}), the solar cell temperature (T_c) and the back surface temperature of the module (T_{bs}) are obtained. The hourly variation of these temperatures from 10:00 to 15:00 areshown in Figure 6.

TABLE 2. Weather condition [19]

Time (h)	Intensity I(t) (W/m^2)	Ambient Temperature(°C)
10:00	641	30.2
10:30	727	31.4
11:00	792	32.0
11:30	816	33.2
12:00	864	34.3
12:30	884	34.6
13:00	880	34.8
13:30	870	36.1
14:00	846	36.0
14:30	800	36.5
15:00	725	35.6

TABLE 3. Some thermo-physical parameters, operating and design parameters [9,12,18]

Parameter	Values
A_{cell}	0.9 m^2
L	2.00 m
b	0.5 m
δ	0.05 m
C_{air}	1005 J/kgK
L_g	0.003 m
K_g	1 W/mK
τ_g	0.95
ε_g	0.88
L_G	0.003
K_G	1 W/mK
τ_G	0.95
α_G	0.04
ε_G	0.88
L_c	0.0003 m
K_c	0.039 W/mK
α_c	0.85
ε_c	0.9
L_T	0.0005 m
K_T	0.033 W/mK
α_T	0.5
L_i	0.05 m
K_i	0.035 W/mK
β_c	0.83
V_w	1 m/s
φ	30
$I_{sc,ref}$	2.98 A
$V_{oc,ref}$	20.5 V
$I_{mp,ref}$	2.76 A
$V_{mp,ref}$	16.3 V
$\mu_{I_{sc}}$	1.325 mA/K
$\mu_{V_{oc}}$	-0.0775 V/K

The outlet air temperature (T_{airout}), the back surface temperature of the module (T_{bs}) and the solar cell temperature (T_c) of model II., glazed PV/T, are higher than the unglazed PV/T due to the reduction in top loss

coefficient (U_t) for the glazed one which is given by Equation (15). With locating a glass cover, the PV contact with the environment is cut and the rate of heat transfer from the top surface of PV decreases. Also, the greenhouse effect in the glazed model is effective on increasing the temperature of solar cell. By increasing the solar cell temperature, the outlet air and the back surface temperatures of the module are increased as well.

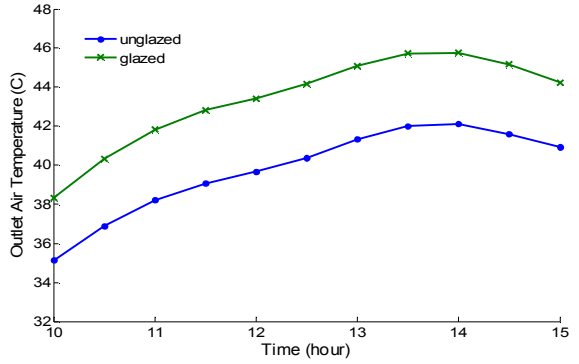

(a)

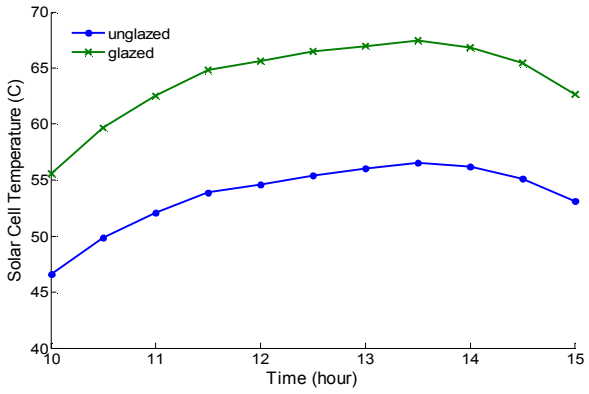

(b)

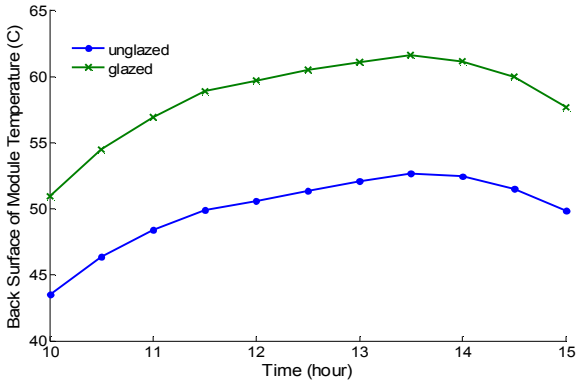

(c)

Figure 6. (a) The hourly variation of outlet air temperature (b) The hourly variation of the solar cell temperature (c) The hourly variation of the back surface temperature

The average difference between the unglazed and glazed states for the outlet air, the solar cell and the back surface temperatures are 3, 10 and 8°C respectively. The hourly variations of thermal efficiencies of the two models are shown in Figure 7. It is obvious that the efficiency of the glazed system is higher than the unglazed one, due to the glass cover effect. The thermal efficiencies of the glazed and unglazed are 42 and 26% respectively. The electrical efficiency of two systems can be compared according to Figure 8. Due to the temperature raising of PV cells in the glazed model, its electrical efficiency is less than the unglazed one. The hourly variations of the overall energy efficiencies of the two models are shown in Figure 9(a). The graph demonstrates that the thermal energy efficiency is more impressive than the electrical efficiency in calculating the overall efficiency. According to the results shown on the figure, the average total efficiency of the unglazed type is 52-53% and of the glazed one has 66-68% efficiency. Figure 9(b) shows the hourly variations of thermal, electrical and overall thermal efficiencies for PV/T which were obtained by Joshi et al. [9]. Considering the trends of the graphs, a good agreement is observed between the obtained results and the mentioned work.

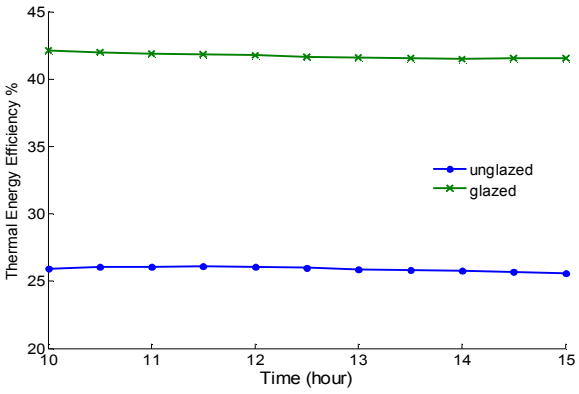

Figure 7. The hourly variation of thermal energy efficiency

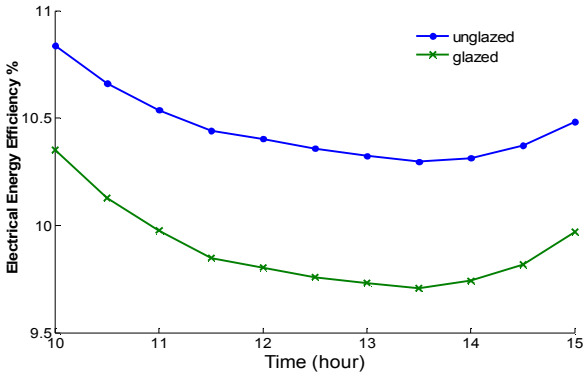

Figure 8. The hourly variation of electrical energy efficiency

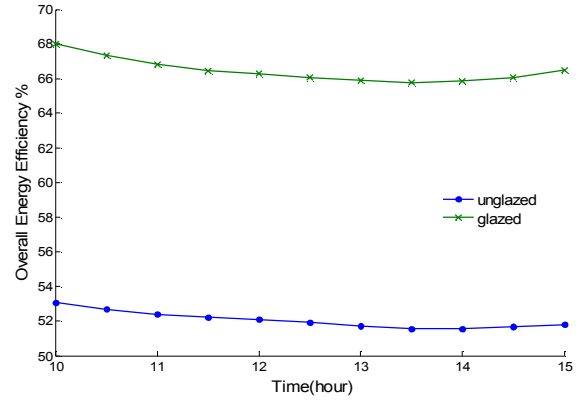

9(a)

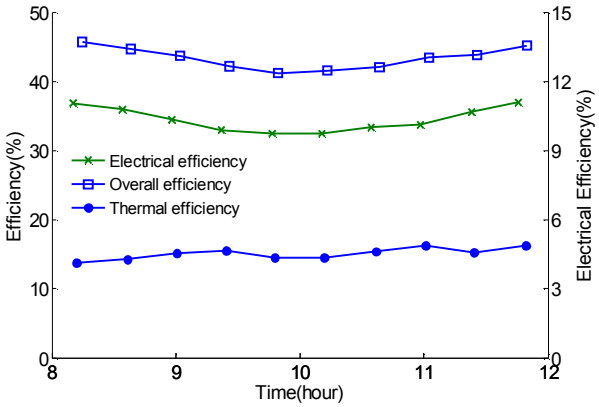

9(b)

Figure 9. (a) Hourly variation of overall energy efficiency at present work (b) Hourly variation of thermal, electrical and overall thermal efficiencies for unglazed glass-to-tedlar hybrid PV/T air collector, Joshi et al. [9]

The hourly variation of exergy efficiency of the two systems indicates that the unglazed system has higher overall exergy efficiency (Figure 10(a)). As it was mentioned in section (4.2), the qualities of the thermal and electrical energies are not the same. Although the glazed system has high thermal and overall energy efficiency but the overall exergy efficiency of unglazed system is high due to production of high quality electrical energy. The exergy efficiency of the glazed system is between 10.5-11.1 and 11.2-11.6% for the unglazed one. The effect of the glazing cover on the exergy efficiency are compatible with the those reported by Chow [14] who investigated this effect on the water PV/T system.

The results of Shahsavari et al. [19] indicate that the exergy efficiencies for the unglazed and glazed models are approximately 9 and 7%, respectively. According to Figure 10(a), the average exergy efficiencies for the unglazed and glazed systems are 11.2 and 10.63%, respectively. Also, the result obtained for exergy efficiency is in conformity with the results of Sarhaddi et al. [18]. In this section, the variation of the overall energy and exergy efficiencies with the mass flow rate and collector length are investigated. The conditions set in this section include solar radiation of 800 Wm^{-2}, ambient temperature of 25°C and wind speed of 1.0 m/s. According to Figure 11(a), it is obvious that the air temperature difference gets less and less with increasing mass flow rate. The validity of the results was checked with Tonui and Tripanagnostopoulos [8].

Increasing the overall energy efficiency with mass flow rate is shown in Figure12(a). The reason of the ascending trend is that the convection heat transfer coefficient, and consequently the rate of heat transfer from PV to the air passing from the channel increases by raising the air mass flow rate. Therefore, the thermal and electrical efficiencies of the studied system increase. Figure12(b) indicates the exergy efficiency variations with mass flow rate. According to the figure in high mass flow rates, the variation of efficiency is low and it almost reaches a steady state condition.

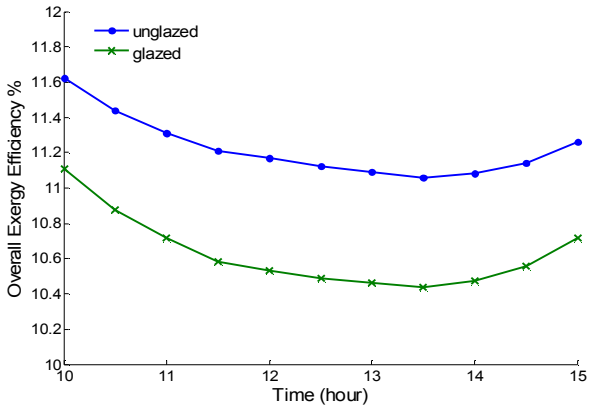

10(a)

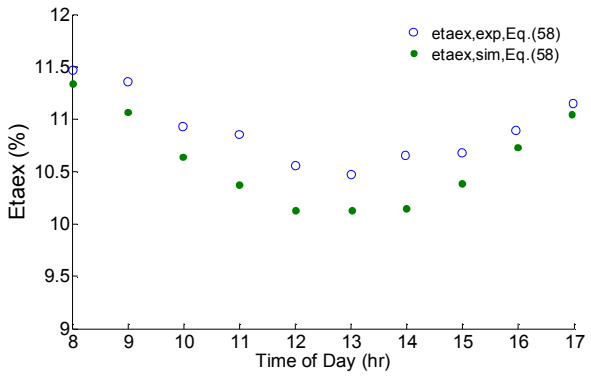

10(b)

Figure 10. (a) The hourly variation of overall exergy efficiency for the current work (b) The simulated and experimental values of exergy efficiency, Sarhaddi et al.[18]

Another parameter which was investigated in this study, was the channel length and the results are reported in Figure 13. According to this figure, the energy and exergy efficiencies decrease with increasing the duct length. With increasing the channel length, the outlet air temperature and the rate of the useful thermal energy gain increase; this raising is accompanied with increasing the system area which both cause efficiency improvement. If the PV/T model is such that the absorbed heat is not proportional with the increase in area, the thermal efficiency will decrease.

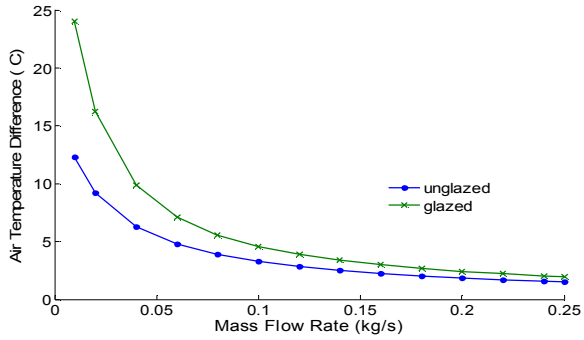

11(a)

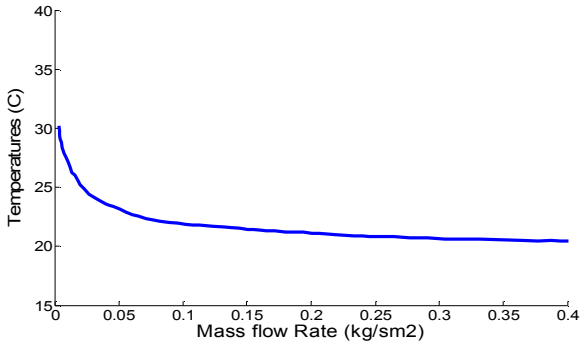

11(b)

Figure 11. (a) Effect of air mass flow rate on the outlet air temperature difference of glazed and unglazed air PV/T (b) Effect of air mass flow rate on the outlet air temperature of unglazed air PV/T, Tonui and Tripanagnostopoulos [8].

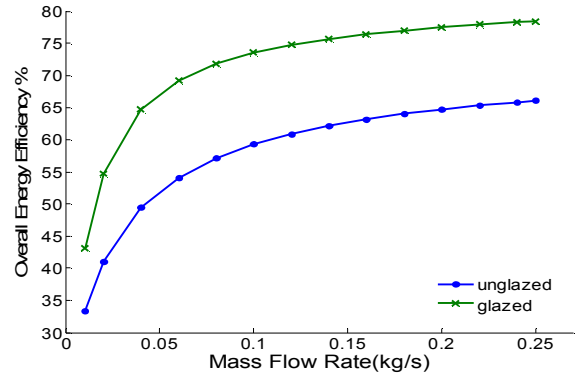

12(a)

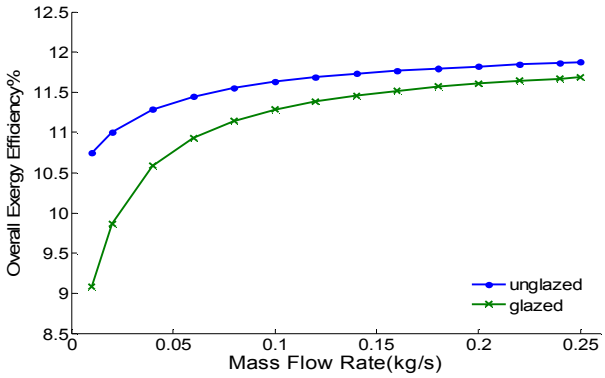

12(b)

Figure 12. (a) Variation of overall energy efficiency with mass flow rate increasing; (b) Variation of overall exergy efficiency with mass flow rate increasing

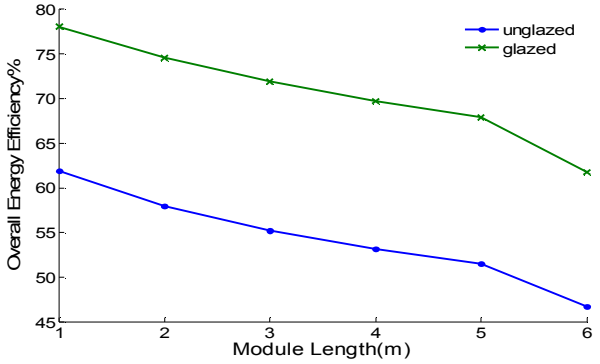

13(a)

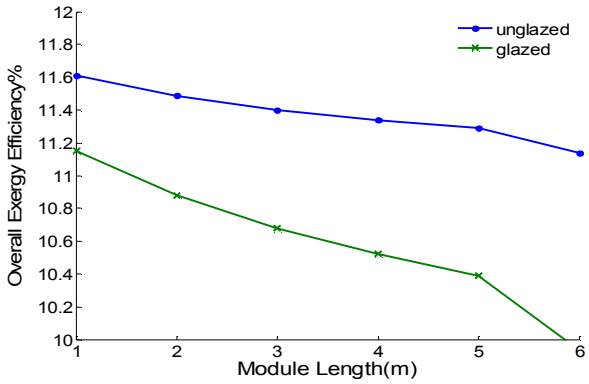

13(b)

Figure 13. (a) Variation of overall energy efficiency with module length; (b) Variation of overall exergy efficiency with module length

By air flowing through the duct, its heat absorbing ability is reduced, the photovoltaic temperature increases and the electrical energy efficiency decreases. According to the electrical and thermal energy

efficiency trends, the overall efficiency decreases. Decreasing the electrical efficiency causes reduction in the electrical exergy efficiency whereas increasing useful energy gain causes thermal exergy efficiency increase. According to these effects, the overall exergy efficiency decrease is indicated in Figure 13. The results shown in Figure 13 are compatibile with those of Joshi et al.[9]. According to the results of Shahsavari et al. [19] there is an optimal channel length (L= 2.76 m) at which the energy efficiency has its highest value, while the exergy efficiency decreases with increasing the channel length.

6. CONCLUSION

In this paper, a numerical study on a forced flow PV/T air collector with both glazed and unglazed positions has been conducted. Since the investigation of exergy for forced convection flow in glazed air PV/T system has not been accomplished yet, we investigated and achieved the following results:

1. Putting glass cover increases the output air temperature and the temperature of photovoltaic modules. Also, this reduces the electrical efficiency.
2. The glazed system has higher thermal and overall energy efficiency than the unglazed ones, where the unglazed ones have higher electrical efficiency.
3. Because of higher electrical efficiency, unglazed system has higher electrical and overall exergy efficiency, while the glazed system has higher thermal exergy efficiency.
4. The overall energy efficiency increases with increasing the mass flow rate and decreases with increasing the length of the module.
5. The overall exergy efficiency increases with increasing the mass flow rate increasing and decreases with increasing the length of the module.
6. Setting glass cover is just suitable in the applications that thermal efficiency has priority over electrical efficiency.

7. REFERENCES

1. Chow, T., "A review on photovoltaic/thermal hybrid solar technology", ***Applied Energy***, Vol. 87, No. 2, (2010), 365-379.
2. Hegazy, A. A., "Comparative study of the performances of four photovoltaic/thermal solar air collectors", ***Energy Conversion and Management***, Vol. 41, No. 8, (2000), 861-881.
3. Zondag, H., De Vries, D. D., Van Helden, W., Van Zolingen, R. and Van Steenhoven, A., "The thermal and electrical yield of a pv-thermal collector", ***Solar energy***, Vol. 72, No. 2, (2002), 113-128.
4. Tiwari, A., Sodha, M., Chandra, A. and Joshi, J., "Performance evaluation of photovoltaic thermal solar air collector for composite climate of india", ***Solar Energy Materials and Solar Cells***, Vol. 90, No. 2, (2006), 175-189.
5. Tiwari, A. and Sodha, M., "Performance evaluation of solar pv/t system: An experimental validation", ***Solar Energy***, Vol. 80, No. 7, (2006), 751-759.
6. Alfegi, E. M. A., Sopian, K., Othman, M. Y. and Yatim, B., "Experimental study on double-pass photovoltaic / thermal solar air collector", in Regional Conference on Engineering Mathematics, Mechanics, Manufacturing and Architecture, Putrajaya, Malaysia, (2007), 71-77.
7. Othman, M. Y., Yatim, B., Sopian, K. and Abu Bakar, M. N., "Performance studies on a finned double-pass photovoltaic-thermal (PV/T) solar collector", ***Desalination***, Vol. 209, No. 1, (2007), 43-49.
8. Tonui, J. and Tripanagnostopoulos, Y., "Air-cooled pv/t solar collectors with low cost performance improvements", ***Solar Energy***, Vol. 81, No. 4, (2007), 498-511.
9. Joshi, A., Tiwari, A., Tiwari, G., Dincer, I. and Reddy, B., "Performance evaluation of a hybrid photovoltaic thermal (PV/T)(glass-to-glass) system", ***International Journal of Thermal Sciences***, Vol. 48, No. 1, (2009), 154-164.
10. Solanki, S., Dubey, S. and Tiwari, A., "Indoor simulation and testing of photovoltaic thermal (PV/T) air collectors", ***Applied Energy***, Vol. 86, No. 11, (2009), 2421-2428.
11. Jin, G. L., Ibrahim, A., Chean, Y. K., Daghigh, R., Ruslan, H., Mat, S., Othman, M. Y., and Sopian, K., "Evaluation of single-pass photovoltaic-thermal air collector with rectangle tunnel absorber", ***American Journal of Applied Sciences***, Vol. 7, No. 2, (2010), 277.
12. Sarhaddi, F., Farahat, S., Ajam, H., Behzadmehr, A. and Mahdavi Adeli, M., "An improved thermal and electrical model for a solar photovoltaic thermal (PV/T) air collector", ***Applied Energy***, Vol. 87, No. 7, (2010), 2328-2339.
13. Joshi, A. S. and Tiwari, A., "Energy and exergy efficiencies of a hybrid photovoltaic–thermal (PV/T) air collector", ***Renewable Energy***, Vol. 32, No. 13, (2007), 2223-2241.
14. Chow, T., Pei, G., Fong, K., Lin, Z., Chan, A., and Ji, J., "Energy and exergy analysis of photovoltaic–thermal collector with and without glass cover", ***Applied Energy***, Vol. 86, No. 3, (2009), 310-316.
15. Tiwari, A., Dubey, S., Sandhu, G., Sodha, M. and Anwar, S., "Exergy analysis of integrated photovoltaic thermal solar water heater under constant flow rate and constant collection temperature modes", ***Applied Energy***, Vol. 86, No. 12, (2009), 2592-2597.
16. Dubey, S., Solanki, S. and Tiwari, A., "Energy and exergy analysis of PV/T air collectors connected in series", ***Energy and Buildings***, Vol. 41, No. 8, (2009), 863-870.
17. Agrawal, S. and Tiwari, G., "Energy and exergy analysis of hybrid micro-channel photovoltaic thermal module", ***Solar energy***, Vol. 85, No. 2, (2011), 356-370.
18. Sarhaddi, F., Farahat, S., Ajam, H. and Behzadmehr, A., "Exergetic performance assessment of a solar photovoltaic thermal (PV/T) air collector", ***Energy and Buildings***, Vol. 42, No. 11, (2010), 2184-2199.
19. Shahsavar, A., Ameri, M. and Gholampour, M., "Energy and exergy analysis of a photovoltaic-thermal collector with natural air flow", ***Journal of Solar Energy Engineering***, Vol. 134, No. 1, (2012).
20. Duffie, J. A. and Beckman, W. A., "Solar engineering of thermal processes", ***NASA STI/Recon Technical Report A***, Vol. 81, (1980), 16591.
21. Petela, R., "Exergy of heat radiation", ***Journal of Heat Transfer***, Vol. 86, (1964), 187.

Energy and Exergy Analysis of Air PV/T Collector of Forced Convection with and without Glass Cover

A. B. Kasaeian[a], M. Dehghani Mobarakeh[b], S. Golzari[a], M. M. Akhlaghi[a]

[a] *Faculty of New Science & Technologies, University of Tehran, Tehran, Iran*
[b] *Research Institute of Petroleum Industry, Tehran, Iran*

P A P E R I N F O

Paper history:
Received 08 December 2012
Received in revised form 06 February 2013
Accepted 28 February 2013

Keywords:
Air PV/T Collector
Energy Efficiency
Exergy Efficiency

چکیده

در این مطالعه، عملکرد کلی سیستم فتوولتائیک/حرارتی هوا-خنک با جریان اجباری هوا بر اساس تحلیل انرژی و اگزرژی مورد بررسی قرار گرفته است. دو ترکیب مختلف از این سیستم که شامل سیستم فتوولتائیک/حرارتی پوشش‌دار و فاقد پوشش می شود، در نظر گرفته شده است. با آنالیز حرارتی و محاسبات عددی صورت گرفته پارامترهای عملکرد سیستم برای شرایط آب و هوایی شهر کرمان بررسی شده است. نتایج به شکل گراف‌هایی ارائه شده و پارامترهایی هم‌چون بازده الکتریکی، بازده گرمایی و بازده کلی این دو نوع ترکیب با هم مقایسه شده است. نتایج نشان می‌دهد بازده گرمایی و بازده کلی انرژی مدل پوشش‌دار بیشتر از مدل بی‌پوشش است، در حالی که بازده الکتریکی و بازده کلی اکسرژی به دست آمده برای مدل بی‌پوشش بیشتر است. بازده کلی انرژی به دست آمده برای مدل‌های پوشش‌دار و بی‌پوشش به ترتیب ٦٦ و ٥٢ درصد و بازده کلی اکسرژی برای مدل پوشش‌دار بین ١٠/٥ و ١١/١ درصد و برای مدل بی‌پوشش ١١/٢ تا ١١/٦ درصد است.

doi: *10.5829/idosi.ije.2013.26.08b.13*